

# Analytical and Numerical Results for the Liquid-Lubricated Magnetic Head-disk Interface Using Measured Rheological Data

Jeffrey L. Streator

G. W. Woodruff School of Mechanical Engineering,  
Georgia Institute of Technology, Atlanta, GA 30332-040

**Abstract**—To increase the information storage density in magnetic disk files, the head, the head-disk spacing must be reduced. This has motivated the investigation of alternatives to the conventional air-lubricated head-disk interface (HDI), which operates at a spacing of about 100 nm. One such alternative under consideration is the liquid-lubricated bearing. To properly model the HDI with a liquid bearing it is necessary to incorporate the rheological properties of liquid lubricants at high shear rates. These rheological properties themselves are most easily measured within the HDI. Recently, some question has arisen in the literature concerning the interpretation of the frictional data acquired in this manner. In this study analytical and numerical solutions of the Reynolds eqn. are applied to the starved, liquid lubricated HDI to provide some validation of the rheological data reported the author and coworkers (Streator *et al.*, 1994). Results of the analysis highlight the importance of the inlet taper region in determining the equilibrium configuration of the starved HDI even when only a small fraction of its length is wetted by the lubricant.

## 1. Introduction

The desire to achieve greater and greater storage densities with magnetic recording disk has motivated the investigation of alternatives to the widely used hydrodynamic air bearing as the means of supporting the read-write head above the disk (Bhushan, 1990). A primary goal of such studies is to reduce the equilibrium spacing between the read-write element and the magnetic medium. In state-of-the-art disk drives, the head-disk spacing is in the neighborhood of 100 nm (Jonsson and Bhushan, 1995). One proposed alternative to the conventional head-disk interface (HDI) involves the use of liquid as the bearing fluid in place of the usual air (Lemke and Frnch, 1992). It has been suggested that the liquid, being of higher viscosity than the air, may allow the attainment of flying heights much below the 100 nm level. The stiffer, more highly damped film should facilitate the achievement of stable flying heights in the near-contact regime (i.e., 20-40 nm).

A few recent reports in the literature attest to the growing interest in assessing the viability of the liquid bearing. De Bruyne and Bogy (1994), investigated the flight dynamics of an HDI with a non-

Newtonian liquid. These authors performed a numerical simulation using a non-Newtonian Bird-Carreau liquid as the bearing fluid. They found that the slider could achieve an equilibrium flying height at 50 nm with a hypothetical lubricant of very low viscosity. Jonsson and Bhushan (1995) performed an experimental investigation of the rheological properties of lubricant films at thicknesses corresponding to the near-contact regime. Streator (1005) introduced the concept of the starved-liquid bearing for the HDI and performed a theoretical investigation of its flying characteristics by employing the narrow-bearing approximation to the Reynolds equation. Chen *et al.* (1996) conducted a numerical simulation of the fully-flooded HDI using measured rheological data. Hsiao *et al.* (1996) performed a theoretical study of pressure generation within the liquid-lubricated HDI using an analytical approximation to the Reynolds equation.

One of the central questions arising in the analysis of the liquid-lubricated HDI relates to the rheology of the lubricant. Because the liquid-lubricated HDI is supposed to operate at sliding speeds in the neighborhood of 10 m/s with lubricant film thicknesses in the 20-40 nm range, the in-

terfacial lubricant is subjected to extremely high shear rates, up to  $10^9/s$ . If the viscosity were to remain at its bulk, low-shear value, one would expect very high shear stresses exerted on the slider. For example, with a lubricant of 10 mPa-s, a sliding speed of 10 m/s and a lubricant film thickness of 20 nm, the predicted shear stress, assuming Newtonian behavior, would be given by:

$$\tau = \frac{\mu U}{h} = \frac{(0.01)(10)}{2 \times 10^{-8}} = 5\text{MPa}$$

For a slider area of 3 mm<sup>2</sup> (typical of a conventional HDI), such a shear stress would result in a friction force of 15 N. Friction forces this high with a liquid film and the given slider area have been reported. In fact, above a certain sliding speed, the measured force can be an order of magnitude or more below what is expected from the Newtonian prediction (Lemke and French, 1992; Streator *et al.*, 1994, Jonnson and Bhushan, 1995). However, while these investigators all observe a reduction in friction force with increasing speed, they do not all attribute the decreasing friction to the same mechanism. Lemke and French (1992) and Streator *et al.* (1994) attribute the drop in friction to a dramatic shear thinning behavior in the lubricant, whereby the lubricant viscosity falls precipitously. On the other hand, Jonnson and Bhushan (1995) suggest that the drop in friction arises because of a sudden decrease in the area of the slider wetted by the lubricant.

The purpose of the present work is to perform both numerical and analytical modeling of the starved HDI in order to shed additional light on the experimental data found in the literature.

## 2. Analysis

In this section we analyze the conditions of equilibrium for the starved, liquid-lubricated HSI. We consider static equilibrium configurations for two-rail sliders with and without an inlet taper.

### 2-1. Starved Liquid Bearing with No Inlet Taper

Fig. 1a provides a schematic of the starved liquid bearing with no inlet taper. (Streator, 1995).

In Fig. 1a,  $l$  is the length of the slider;  $l_p$  is the distance from the leading edge of the slider to the pivot point, P, (where the slider is spring-loaded);  $\theta$  measures the slider pitch angle;  $d$  is the distance

from the slider rail location to the pivot point; and  $l_s$  is the length along the slider which is "starved" of lubricant. The width of each rail is denoted by  $b$ . The inlet film thickness is denoted by  $h_i$ , the exit film thickness by  $h_o$ , while the film thickness at the edge of the taper is denoted by  $h_1$ . The local sliding speed is labeled  $U$ . We note here that Fig. 1a is not to scale. For a typical liquid-lubricated bearing, the length of the slider is about 100,000 times the minimum film thickness, and the slider pitch angle is generally less 1  $\mu$ rad.

It is noted that Fig. 1a shows a starved HDI with a two-rail slider geometry, whereas the original concept of Lemke and French, employed a four-pad

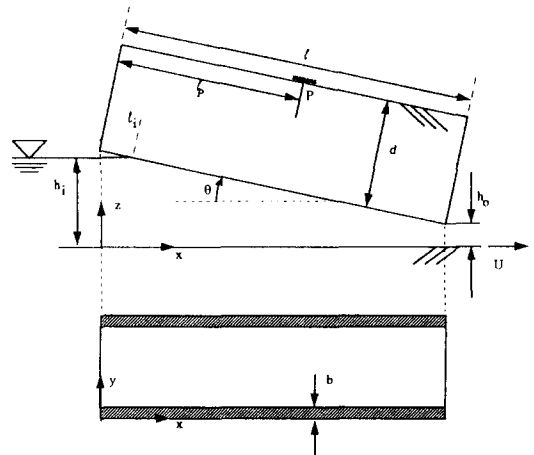


Fig. 1a. Schematic of a starved liquid bearing for the HDI without an inlet taper.

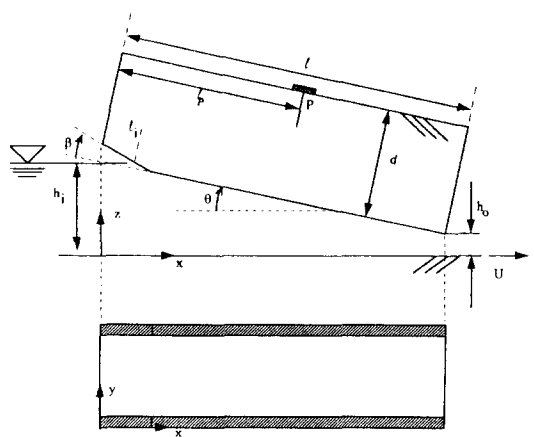


Fig. 1b. Schematic of a starved liquid bearing for the HDI with an inlet taper.

slider geometry (Lemke and French, 1992) and a fully-flooded bearing. With the fully-flooded HDI, an excess of lubricant is maintained on the disk. The flying height is then governed by the balance of the forces and moments exerted on the slider. In contrast, the starved bearing (Fig. 1a) has a film thickness that is assumed equal to the thickness of the applied lubricant film and the degree of starvation represents a parameter to be determined.

Although conventional sliders do indeed have an inlet taper (see Fig. 1b), the taperless slider might be expected to model the HDI well when the lubricant film thickness is in the 20-40 nm range. If is assumed that the height of the lubricant film does not exceed by very much the applied film thickness, then only a very small length of the inlet taper is wet by the lubricant. For example, with a inlet taper angle of 0.01 radians, a maximum (inlet) film thickness of 30 nm, and a minimum (outlet) film thickness of 25 nm, the wetted portion of the inlet taper is approximately  $5 \text{ nm}/0.1 = 0.5 \text{ } \mu\text{m}$ . Comparing this value with typical length for the "flat" portion of the bearing, say 2.0 mm, we conclude that the wetted length of the taper region accounts for only 0.025% of the entire wetted length of the slider. Ignoring the effects of this small region would than lead to the taperless geometry of Fig. 1a as the model for the lubricated interface.

Pressure development within the lubricant film is governed by the Reynolds equation:

$$\frac{\partial}{\partial x} \left( \frac{h^3}{\mu} \frac{\partial \rho}{\partial x} \right) + \frac{\partial}{\partial y} \left( \frac{h^3}{\mu} \frac{\partial \rho}{\partial y} \right) = 6u \frac{dh}{dx} \quad (1)$$

Here is assumed that the film thickness varies only in the x-direction, and that each slider rail acts identically.

Following Streator (1995), one can employ the narrow-bearing approximation to the Reynolds eqn. since the slider aspect ratio,  $b/l$ , is low and the slider pitch angle is expected to be small. In this approximation, one neglects the Poiseuille component of flow in the sliding direction in favor of the Poiseuille component of flow in the transverse direction, thereby eliminating the first term of (1). Once this approximation is made one can readily solve for the pressure distribution as:

$$p(x, y) = \frac{3\mu U}{h^3} \frac{dh}{dx} (y^2 - yb) \quad (2)$$

In Streator (1995) this pressure distribution was used to determine the various forces and moments exerted on the slider. The imposition of and force balance led to the determination of the equilibrium starvation length  $l_s$ , and pitch angle  $\theta$  in terms of the operating conditions. The resulting expressions are given by:

$$\frac{l_s}{l} = \frac{\frac{2l_p}{l} - 1 - \frac{4bd}{W} \left( \frac{\alpha\mu_o U}{h_o} \right)^n}{1 - \frac{4bd}{W} \left( \frac{\alpha\mu_o U}{h_o} \right)^n}, \quad \theta = \frac{h_i - h_t}{l - l_s} \quad (3)$$

where  $W$  is the external load,  $\mu_o$  is the nominal (low-shear) lubricant viscosity and  $\alpha$  and  $n$  are parameters determined from rheological measurements (Streator, 1995). The physical interpretation of the rheological parameters is made clear by the empirical relation:

$$\tau = \left( \alpha \frac{\mu_o U}{h} \right)^n \quad (4)$$

When the liquid has a Newtonian response, then  $\alpha = 1$  and  $n = 1$ . In the so-called "rupture" of lubrication (Streator et al., 1994) with a certain class of perfluoropolyether (PFPE) liquids,  $\alpha = 1.13 \times 10^{-5}$  and  $n = -0.58$  in SI units.

If the interpretation of equation (3) it is assumed that the minimum film thickness,  $h_o$  is equal to the applied lubricant film thickness (Streator, 1995) From equation (3), it is readily seen that the starvation length,  $l_s$ , is sensitive to the placement of the pivot point,  $P$ , via the parameter,  $l_p$ . Equation (3), indicates that when  $l_p/l = 0.5$ , the starvation is always negative which is not allowed on physical grounds. The interpretation of a negative value of starvation length as calculated by (3), is that the slider cannot maintain equilibrium at the applied thickness,  $h_o$  under the given operating conditions.

That a negative starvation length is predicted when  $l_p/l$  equals 0.5 is surprising in that most sliders are fabricated with a pivot point centered over the slider length yet they are found experimentally to "fly" at the applied film thickness even at thicknesses where only a very small length of the inlet taper is expected to be wetted (Streator et al., 1994).

The disparity between the theoretical prediction of (3) and the experimental observations suggest the ef-

fect of the small wetted of the inlet taper cannot be neglected. Static equilibrium for a slider an inlet taper is considered in the next section.

### 2-2. Starved Liquid Bearing with an Inlet Taper

The starved liquid bearing with an inlet taper in Fig. 1b. When the lubricant is assumed to interact with the inlet taper over some finite length, it can be shown that the narrow-bearing approximation is no longer an accurate model for the pressure buildup beneath the bearing. This result stems primarily from the large change in slope between the inlet region and the exit region. Hence we perform a numerical solution of (1).

A standard finite difference technique is used to determine the pressure distribution beneath the slider (see Chen *et al.*, 1996, for details of the details of the method). Once the pressure distribution is determined, a balance of forces and moments is imposed to determine the equilibrium starvation length and pitch angle corresponding to the applied film thickness. In the force balance equation, the hydrodynamic force of the liquid lubricant must be equal in magnitude to the external load. In the moment balance equation, the frictional moment about the slider pivot must be countered by a hydrodynamic due to the support flexure is neglected owing to the assumed small spring constant and very small slider pitch angles).

### 3. Simulation Parameters

Table 1 provides the parameter values with which each of the numerical simulations in performed.

Using the above data, simulations are performed for cases involving sliding speeds of 0.12 and 12 m/s. The lowest speed corresponds to a sliding speed

**Table 1. Conditions common to each of the numerical simulations**

Parameter	Value
slider length, $l$	4.00 mm
rail width, $b$	0.4 mm
vertical pivot position, $d$	0.8 mm
horizontal pivot position, $l_p$	2.0 mm
external load, $W$	0.15 N
applied lubricant film thickness, $h_0$	25.1 nm
nominal lubricant viscosity, $\mu_0$	0.054 Pa-s

below the onset of the rupture regime of Streator *et al.* (1994). For this case, the lubricant is assumed to respond in a manner consistent with the rheological data of Cantow *et al.* (1986), as described by Streator *et al.* (1994). For the higher sliding speed (12 m/s), equation (4) is applied using the empirical values of  $\alpha$  and  $n$  indicated above, and computations are performed for sliders with and without an inlet taper. In determining the slider equilibrium configuration, the slider, pitch angle,  $\theta$ , and the starvation length,  $l_s$ , are adjusted until force-and-moment balance is achieved.

### 4. Results and Discussion

Fig. 2 shows the computed center-line pressure profile for a static equilibrium configuration. The solid circles show results for the case when the sliding speed is 0.12 m/s while the open triangles correspond to a sliding speed of 0.12 m/s. Based on the rheological measurements of Streator *et al.* (1994), the lower sliding speed corresponds to operation in a mild shear-thinning regime while the higher speed corresponds to operation in the "rupture" regime, where the measured friction forces are found to decay as the sliding speed is increased. The figure legend also indicates the equilibrium starvation length,  $El_s$ , for each case. The peak pressure buildup in the inlet is lower for the higher sliding speed because of the lower lubricant viscosity experienced in the rupture regime.

Although not indicated in the figure, the friction force for the lower sliding speed (i. e., prior to rupture) is 440 mN. Such a large friction force produces a substantial moment about the slider pivot

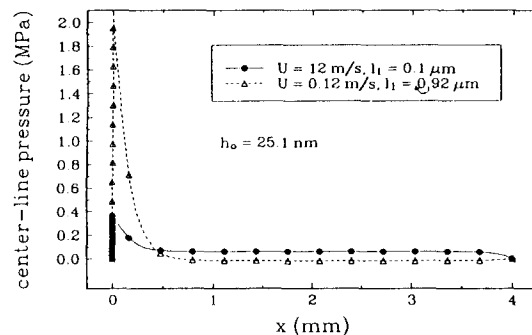


**Fig. 2. Center-line pressure profile for two static equilibrium slider configurations.**

point. At slider equilibrium this moment must be balanced by the action of the resultant load-the-torsional spring stiffness being assumed negligible. Note that the pressure profile goes from large positive values to slightly negative ones, which is consistent with the clockwise moment needed to balance the counterclockwise frictional moment (see Fig. 1b). The negative values in pressure result from a equilibrium pitch angle,  $\theta$  that is slightly negative-it is  $-0.14$  nrad for this case.

These results suggest that the slider can maintain static equilibrium in the face of a substantial frictional moment. As the slider tends to tip counterclockwise, the slider pitch angle  $\theta$  becomes negative and the pressure in the "flat" section of the bearing becomes negative. The achievement of equilibrium is further enabled by the action of the inlet taper which generates large inlet pressures even when only a small portion of the taper is wetted by the lubricant (i.e.,  $l_1 = 0.092 \mu\text{m}$ ).

The foregoing result addresses an objection raised by Jonnson and Bhushan (1995), concerning the interpretation of friction measurements by Streater *et al.* (1994). The moment balance analysis of Jonnson and Bhushan (1995) suggests that the slider must tip (counterclockwise) completely onto its inlet taper region when the frictional force becomes greater than about 100 mN. Although their own measurements indicate peak friction forces close to 1 N, they argue that the subsequent drop in friction observed with increased sliding velocities is due to slider tipping. In contrast, the results for  $U = 0.12$  m/s in Fig. 2 provide explanation as to why liquid-lubricated HDI frictional forces can be measured that greatly exceed

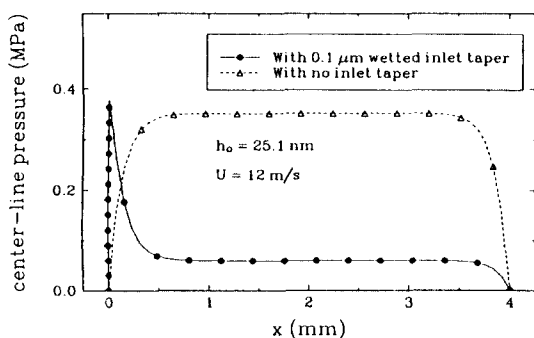


**Fig. 3. Center-line pressure profiles for identical operating conditions (including pitch angle) but with and without an inlet taper.**

the theoretical limit of Jonnson and Bhushan (1995).

Fig. 3 shows the center-line pressure profiles for a sliding speed of 12 m/s with and without the inlet taper. The graph with the solid is the same curve that appears in Fig. 2 and corresponds to a static equilibrium condition. The curve with open triangles shows the pressure profile that results from the identical operating conditions and pitch angle and as the other curve but without any inlet taper. This figure clearly illustrates the importance of including the small wetted region of the inlet taper in the determination of the pressure profile.

## 5. Conclusion

This study considered both analytical and numerical solutions of the starved liquid lubricate HDI. Results of the study indicate that:

(1) The inlet taper plays an important role in the development of the pressure distribution in the starved HDI even when only a small portion of it is wetted by the lubricant.

(2) The head-disk interface can maintain static equilibrium without tipping of the slider even when large frictional moments arise.

## References

1. Bhushan, B., "Tribology and Mechanics of Magnetic Storage Media," Springer-Verlag, 1990.
2. Cantow, M. J. R., Ting, T. Y., Barrall, E. M., Porter, R. S., and George, E. R., "Shear Dependence of Viscosity for Perfluoropolyther Fluids," *Rheo. Acta.*, Vol. 25, pp. 69-71, 1986.
3. De Bruyne, F. A., and Bogy, D. B., "Numerical of the Lubrication of the Head-Disk Interface Using a Non-Newtonian Fluid," *Journal of Tribology, Trans. ASME*, Vol. 116, no. 3, pp. 541-548, 1994.
4. Hsiao, H.S., Bhushan, B., and Hamrock, H., "Ultrathin Liquid Lubrication of Magnetic Head-Rigid Disk Interface for Near-Contact Recording: Part I-A Cosed-Form Solution to the Reynolds Equation," *Journal of Tribology, Trans. ASME*, (in press).
5. Jonnson, U. and Bhushan, B., "Measurement of Rheological Properties of Ultrathin Lubricant Films at Very High Shear Rates and Near-Ambient Pressure," *Journal of Applied Physics*, Vol., 78, no. 5, pp. 3107-3114, 1995.
6. Lemke, J. U., and French, W. W., "Information Re-

- ording Apparatus with a Non-Newtonian Liquid Bearing," U. S. Patent NO. 5,097, 368, Mar. 17, 1992.
7. Streator, J. L., "Head-Disk Interface Performance with a Starved Liquid Bearing: Analytical Solution to Reynolds Equation in the Near-Contact Regime," *Journal of Tribology*, Trans ASME, (in press).
  8. Streator, J. L., Gerhardstein, J. P., and McCollum, C. B., "The Low-Pressure Rheology of Ultra-Thin Lubricant Films and its Influence on Sliding Contact," *ASME Journal of Tribology*, Vol. 116, no. 1, pp. 119-126, 1994.
  9. Chen, P., McCollum, C. B., and Streator, J. L., "Numerical Analysis of the Fully-Flooded Magnetic Head-Disk Interface Using Measured Rheological Data," *ASME Journal of Tribology*, (submitted), 1996.